

Electronic Supplementary Information for

A High Capacity Thiospinel Cathode for Mg Batteries

Xiaoqi Sun^a, Patrick Bonnicks^a, Victor Duffort^a, Miao Liu^b, Ziqin Rong^c, Kristin A. Persson^b, Gerbrand Ceder^d, and Linda F. Nazar^{*a}

- a) Department of Chemistry and the Waterloo Institute of Nanotechnology, University of Waterloo, Waterloo, Ontario N2L 3G1, Canada
- b) Applied Energy Materials Group, Lawrence Berkeley National Laboratory, CA 94720, United States
- c) Department of Materials Science and Engineering, Massachusetts Institute of Technology, Cambridge, MA 02139, United States
- d) Materials Science Division, Lawrence Berkeley National Laboratory, Berkeley, CA 94720, United States

E-mail: lfnazar@uwaterloo.ca

Experimental Section

Material synthesis and characterization. Cubic “C-Ti₂S₄” was synthesized by previously reported procedures.^{1,2} X-ray diffraction (XRD) analysis was carried out on a PANalytical Empyrean diffractometer with Cu-K α radiation in Debye-Scherrer geometry using samples sealed in a 0.3 mm capillary. Rietveld refinement³ was performed using the FullProf suite⁴. Scale factor, zero point, background, lattice parameters, fractional coordinates, occupancies, and the Ti and S thermal parameters were sequentially refined in C-Ti₂S₄ (**Table S2a**). The refined occupancy on sulfur (0.99(4)) was very close to one, and was thus set to 1.0. The thermal parameter for the trace Cu in the 8a site was fixed at the previously reported value of $B_{\text{iso}} = 1.0$.⁵

In the discharged material, the occupancies and thermal parameters of Cu, Ti and S were initially fixed with their values from C-Ti₂S₄. Fourier mapping revealed electron density on both 8a and 16c sites, and therefore Mg was introduced on these sites. Owing to the well-known interplay between site occupancy and atomic displacement parameter for a given site, the thermal parameter for 16c was fixed at $B_{16c} = 1.0$ (based on an average of literature values)⁶, and $B_{8a} = 1.0$ for the 8a site constrained with Cu in order to better refine the occupancy. The occupancies were then re-refined using B_{iso} values between 0.5 to 1.5 (see below, **Table S3**), showing they did not differ significantly and verifying the validity of this approach. In the charged and intermediately discharged samples, Mg was only found on the 16c site (**Table S2c, S4 and S5**); but none on the 8a site.

Material morphologies were examined using a Zeiss field emission scanning electron microscope (SEM) equipped with an energy dispersive X-ray spectroscopy detector (EDX).

Electrochemistry. Electrode preparation and cell assembly was carried out in an Ar-filled glovebox where O₂ and H₂O levels were kept below 5 ppm. Positive electrodes were prepared by mixing the as-prepared materials with Super P and polyvinylidene fluoride (PVDF, Sigma-Aldrich, average Mw ~ 534,000) in a 8:1:1 weight ratio in N-methyl-2-pyrrolidone (NMP, Sigma-Aldrich, 99.5%) and casting the slurry onto Mo foil. The APC electrolyte was synthesized following the reported procedure,⁷ with tetrahydrofuran (THF) or tetraglyme (G4) as the solvent. Magnesium metal was polished with carbide paper (Mastercraft[®], 180 grit SiC) and cleaned prior to use. Coin cells (2325) with Mg counter electrodes were used for cycling studies. All electrochemistry was performed with a VMP3 potentiostat/galvanostat (Bio-logic), with cells held in a thermostatted oven at 60°C.

Galvanostatic Intermittant Titration Technique (GITT) experiments were performed at 60°C using a 3-electrode ConFlat cell⁸ with Mg foil reference and counter electrodes. Each current-on period used a C/200 (59.3 uA) rate and lasted for 2.5 hours. The subsequent current-off period was terminated when dE/dt (the slope) had decreased to 0.1 mV/h. During each current-on period, the potential from about $t = 25$ s to 400 s was plotted against \sqrt{t} , and the slope ($dE/d\sqrt{t}$) was extracted. This $dE/d\sqrt{t}$ value can be used in concert with the slope of the equilibrium potential curve (dE/dx), shown in Figure 4b of the text, to calculate the chemical diffusion coefficient using Equation 1:⁹

$$D = \left(\frac{4}{\pi}\right) \left(\frac{IV_M}{nFS}\right)^2 \left(\frac{\frac{dE}{dx}}{\frac{dE}{d\sqrt{t}}}\right)^2. \quad [1]$$

Here, V_M is the molar volume, n is the number of electrons transferred per mole of Mg, F is Faraday's constant, S is the surface area exposed to electrolyte, D is the chemical diffusion coefficient, dE/dx is the slope of the equilibrium potential curve at the present potential, I is the current and $dE/d\sqrt{t}$ is derived from the potential vs time data. This chemical diffusion coefficient can then be converted into a so-called self-diffusion coefficient using Equation 2:⁹

$$D = -\frac{nq_e x}{kT} \frac{dE}{dx} D_{Mg}. \quad [2]$$

Here, k is Boltzmann's constant, T is the temperature, n is the number of electrons transferred, q_e is the charge of an electron, x is the present value in $Mg_xTi_2S_4$ and dE/dx is the same as before. Finally, these self-diffusion coefficients can be converted to diffusion energy barriers (E_m) using the Arrhenius-style relationship of Equation 3:

$$E_m = -kT \ln\left(\frac{2D_{Mg}}{\nu a^2}\right). \quad [3]$$

Here, 2 is the number of directions Mg can hop from an octahedral site in the spinel structure, ν was approximated to be 10^{13} Hz, and ' a ' is the hopping distance, which is about 2.25 \AA in spinel Ti_2S_4 .

First Principles Calculations. The calculations were performed using the standard Materials Project parameters, using Density Functional Theory as implemented in the Vienna ab initio software package (VASP). The projector augmented-wave (PAW) method was used to describe the wavefunctions near the core and the generalized gradient approximation (GGA) within the Perdew–Burke–Ernzerhof (PBE) parameterization was employed as the electron exchange–correlation functional. Possible Mg configurations were generated by enumerating all possible configurations within a $2 \times 2 \times 2$ spinel unit cell and ranked by their electrostatic energy. Only the first several of configurations on the ranking list are calculated at each composition. All magnetic ions were initialized ferromagnetically and the cell shape, volume and atomic positions are fully optimized throughout this work.

Formation energies for each configuration in **Fig 3a** are calculated as:

$$\Delta E_f = E(\text{Mg}_x\text{Ti}_2\text{S}_4) - x E(\text{MgTi}_2\text{S}_4) - (1-x) E(\text{Ti}_2\text{S}_4) \quad [4]$$

where $E(\text{MgTi}_2\text{S}_4)$ is the lowest energy state at the composition MgTi_2S_4 and $E(\text{Ti}_2\text{S}_4)$ is the energy of the empty Ti_2S_4 spinel. The formation energy is given for states with only octahedral Mg occupancy, only tetrahedral occupancy, and for states with mixed occupancy. Note that as the energy is normalized per formula unit of Ti_2S_4 , the contribution of Mg to the energy differences between various configurations, increases with x in the plot. As a result, the increased energy difference between the states with octahedral and tetrahedral occupancy does not necessarily indicate any change of the Mg site energy. While the enumeration of all configurations in the $2 \times 2 \times 2$ spinel cell leads to a large number of possible configurations, it cannot be excluded that the lowest energy for all composition is not found with this procedure. Only with substantially more exhaustive and elaborate techniques such as cluster expansions paired with Monte Carlo anneals, can a broader search for the most stable configurations be attempted.

Mg and Li migration energies were calculated using the nudged elastic band (NEB) method.¹⁰ The convergence threshold of the total energy was set to 1×10^{-5} eV, and a tolerance of 0.1 eV/Å for the forces was used to converge the minimum energy path (MEP) in the NEB procedure. The initial MEPs were prepared by linear interpolation between the end-points. In order to avoid spurious interactions between images, supercells of appropriate sizes were used ensuring a minimum inter-image distance of 8 Å.

List of Supplementary Tables

Table S1. EDX results for C -Ti₂S₄

Sample	Pristine	Discharged	Charged
EDX	Cu _{0.09(2)} Ti ₂ S _{3.57(8)}	Mg _{0.79(7)} Cu _{0.10(2)} Ti ₂ S _{3.69(9)}	Mg _{0.084(4)} Cu _{0.127(9)} Ti ₂ S _{3.91(6)}

Table S2a. Refined parameters for de-copperiated C-Ti₂S₄ (space group = Fd $\bar{3}$ m, $a = 9.77584(9)$ Å, $\chi^2 = 4.60$, Bragg R-factor = 5.23). The resulting formula Cu_{0.112(3)}Ti₂S₄ is described as Cu_{0.1}Ti₂S₄ throughout the text for clarity.

Atom	Wyck.	x	y	z	Occ.	B _{iso} (Å ²)
Cu	8a	0.125	0.125	0.125	0.112(3)	1.0
Ti	16d	0.5	0.5	0.5	1.00	1.05(2)
S	32e	0.25161(5)	0.25161(5)	0.25161(5)	1.00	0.80(2)

Table S2b. Refined parameters for **discharged** C-Ti₂S₄ (Echem = Mg_{0.84}/C-Ti₂S₄, refined = Mg[oct]_{0.59(1)}Mg[tet]_{0.189(7)}Cu_{0.1}Ti₂S₄, space group = Fd $\bar{3}$ m, $a = 10.0971(4)$ Å, $\chi^2 = 5.67$, Bragg R-factor = 3.12).

Atom	Wyck.	x	y	z	Occ.	B _{iso} (Å ²)
Cu	8a	0.125	0.125	0.125	0.112	1.0
Ti	16d	0.5	0.5	0.5	1.00	1.05
S	32e	0.2551(1)	0.2551(1)	0.2551(1)	1.00	0.80
Mg1	8a	0.125	0.125	0.125	0.189(7)	1.0
Mg2	16c	0	0	0	0.296(5)	1.0

Table S2c. Refined parameters for the **charged** C -Ti₂S₄ (Echem = Mg_{0.03}/C-Ti₂S₄, refined = Mg[oct]_{0.016(6)}Cu_{0.1}Ti₂S₄, space group = Fd $\bar{3}$ m, $a = 9.8060(3)$ Å, $\chi^2 = 5.73$, Bragg R-factor = 4.42).

Atom	Wyck.	x	y	z	Occ.	B _{iso} (Å ²)
Cu	8a	0.125	0.125	0.125	0.112	1.0
Ti	16d	0.5	0.5	0.5	1.00	1.05
S	32e	0.25296(5)	0.25296(5)	0.25296(5)	1.00	0.80
Mg	16c	0	0	0	0.008(3)	1.0

Table S3. Mg occupancies obtained with different fixed thermal parameters in discharged C-Ti₂S₄.

B _{iso} (Å ²)	Mg1 (8a)	Mg2 (16c)	χ ²	R _{Bragg}
0.5	0.192(7)	0.291(5)	5.50	2.84
0.8	0.190(7)	0.294(5)	5.59	3.00
1	0.189(7)	0.296(5)	5.67	3.12
1.2	0.187(7)	0.298(5)	5.73	3.23
1.5	0.186(7)	0.300(5)	5.82	3.44

Table S4. Refined parameters for the **partially discharged** material (Echem = Mg_{0.43}/C-Ti₂S₄, refined = Mg[oct]_{0.378(8)}Cu_{0.1}Ti₂S₄, space group = Fd $\bar{3}$ m, a = 9.9244(2) Å, χ² = 4.65, Bragg R-factor = 3.86).

Atom	Wyck.	x	y	z	Occ.	B _{iso} (Å ²)
Cu	8a	0.125	0.125	0.125	0.112	1.0
Ti	16d	0.5	0.5	0.5	1.00	1.05
S	32e	0.25389(5)	0.25389(5)	0.25389(5)	1.00	0.80
Mg	16c	0	0	0	0.189(4)	1.0

Table S5. Refined parameters for the **partially discharged** material (Echem = Mg_{0.6}/C-Ti₂S₄, refined = Mg[oct]_{0.526(8)}Cu_{0.1}Ti₂S₄, space group = Fd $\bar{3}$ m, a = 9.9808(2) Å, χ² = 3.04, Bragg R-factor = 3.47).

Atom	Wyck.	x	y	z	Occ.	B _{iso} (Å ²)
Cu	8a	0.125	0.125	0.125	0.112	1.0
Ti	16d	0.5	0.5	0.5	1.00	1.05
S	32e	0.25411(5)	0.25411(5)	0.25411(5)	1.00	0.80
Mg	16c	0	0	0	0.263(4)	1.0

List of Supplementary Figures

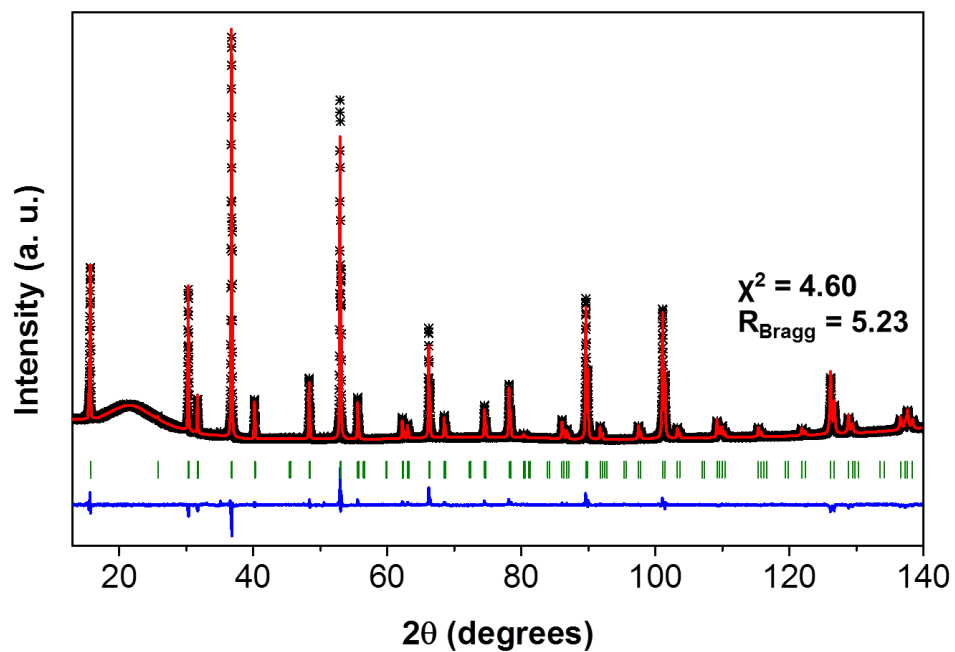


Fig. S1 XRD Rietveld refinement fit of $\text{Cu}_{0.1}\text{Ti}_2\text{S}_4$. (Black crosses – experimental data, red lines – fitted data, blue line – difference map between observed and calculated data, green ticks – the $\text{Fd}\bar{3}\text{m}$ spinel phase). The broad hump is a background signal from the X-ray capillary.

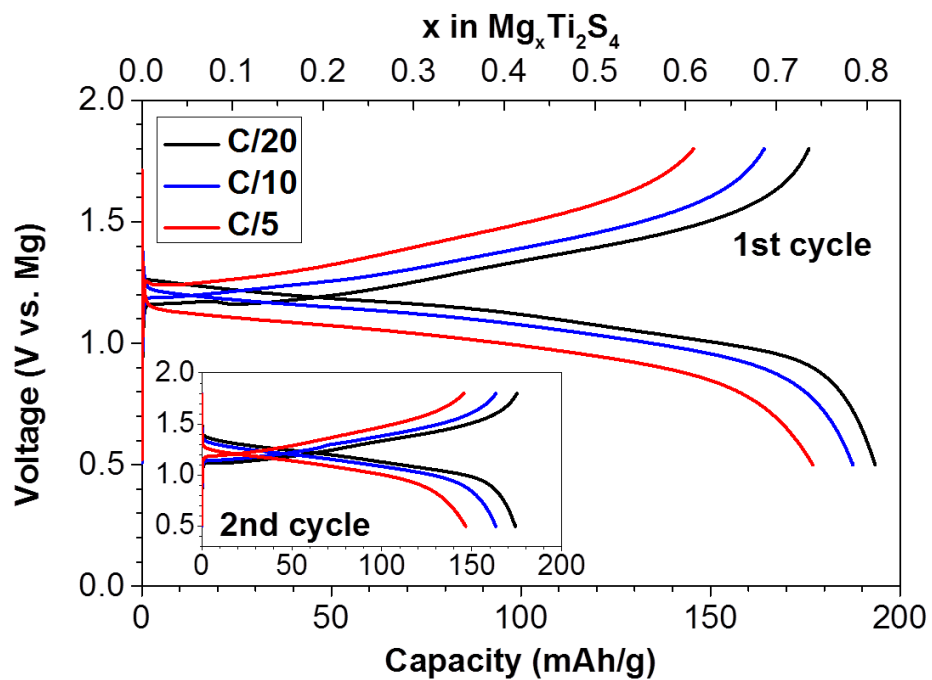


Fig. S2 Electrochemistry of C-Ti₂S₄ coin cells using an APC/G4 electrolyte and a Mg negative electrode at 60°C.

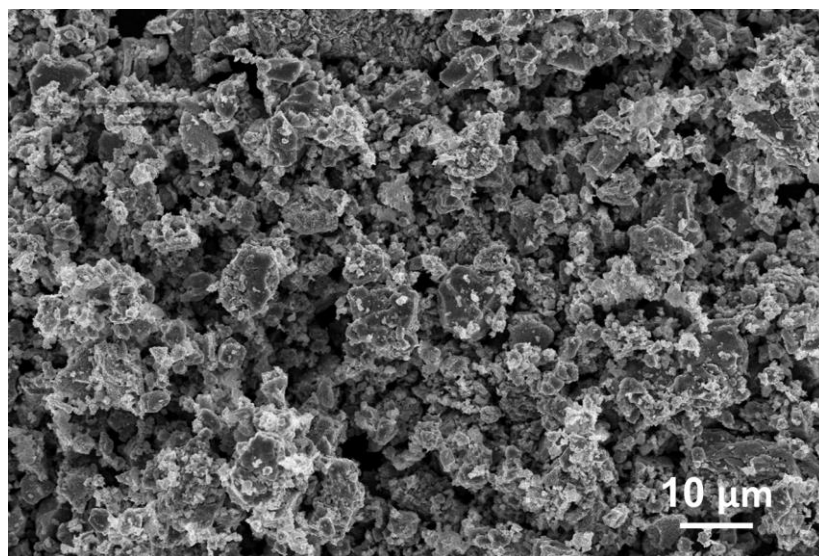


Fig. S3 SEM image of de-copperiated $\text{Cu}_{0.1}\text{Ti}_2\text{S}_4$ (C- Ti_2S_4).

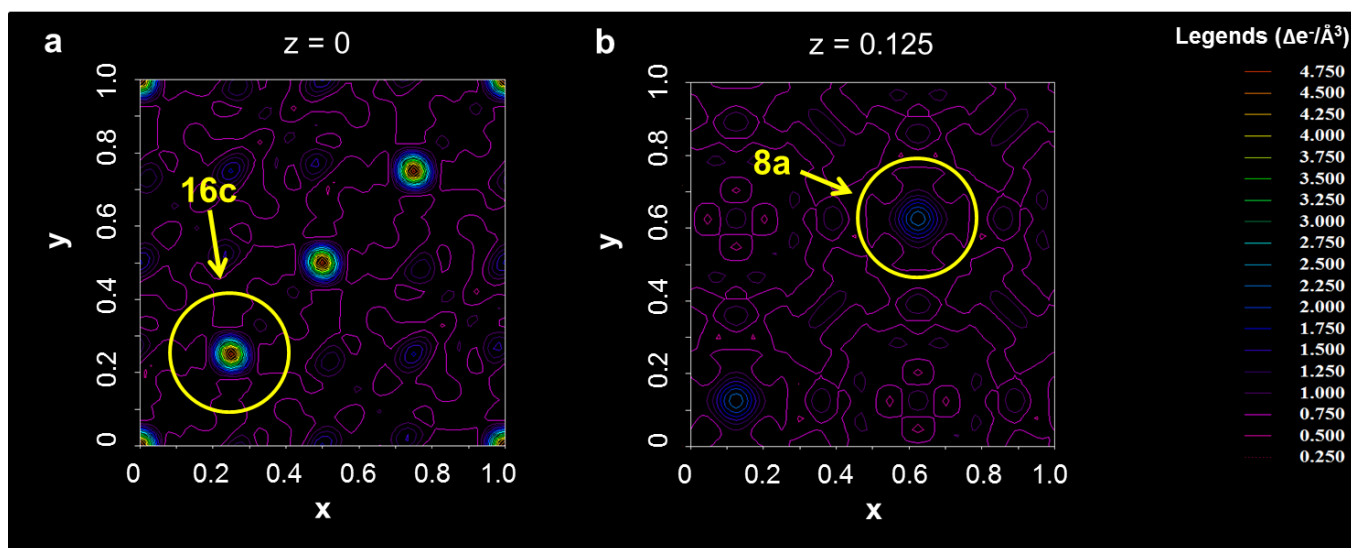


Fig. S4 Fourier maps of the discharged XRD pattern with only Cu, Ti, S in the structure, showing the missing electron density on the (a) 16c and (b) 8a site in the absence of Mg occupation.

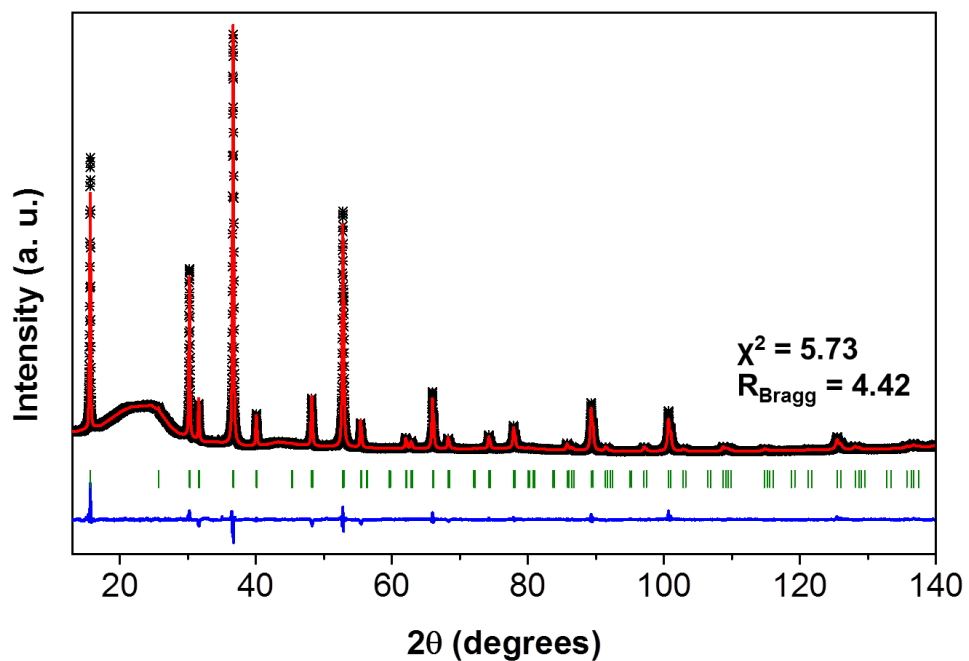


Fig. S5 XRD Rietveld refinement fit of charged $\text{Mg}_{0.02}\text{Cu}_{0.1}\text{Ti}_2\text{S}_4$. (Black crosses – experimental data, red lines – fitted data, blue line – difference map between observed and calculated data, green ticks – the $\text{Fd}\bar{3}\text{m}$ spinel phase). The broad hump is a background signal from the X-ray capillary.

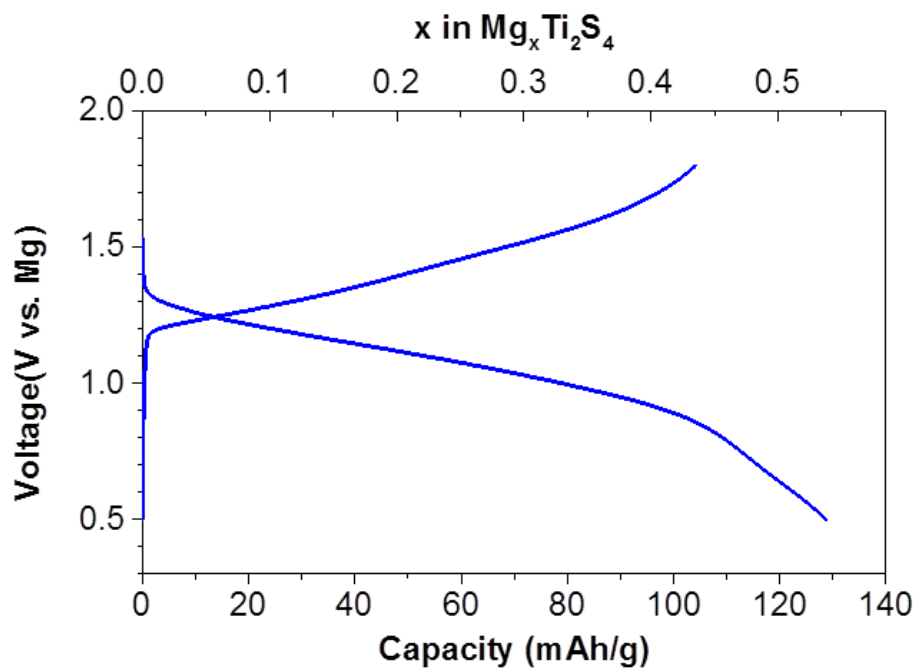


Fig. S6 First cycle of C-Ti₂S₄ coin cell with an APC/THF electrolyte and a Mg negative electrode at C/50 and room temperature.

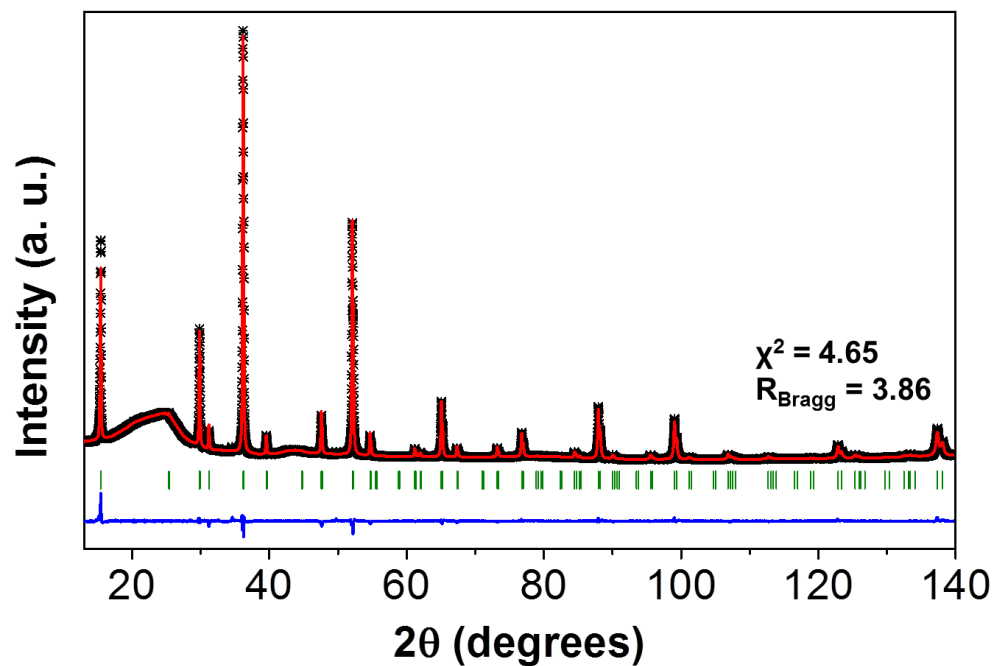


Fig. S7 XRD Rietveld refinement fit of partially discharged $\text{Mg}_{0.4}\text{Cu}_{0.1}\text{Ti}_2\text{S}_4$. (Black crosses – experimental data, red lines – fitted data, blue line – difference map between observed and calculated data, green ticks – the $Fd\bar{3}m$ spinel phase). The broad hump is a background signal from the X-ray capillary.

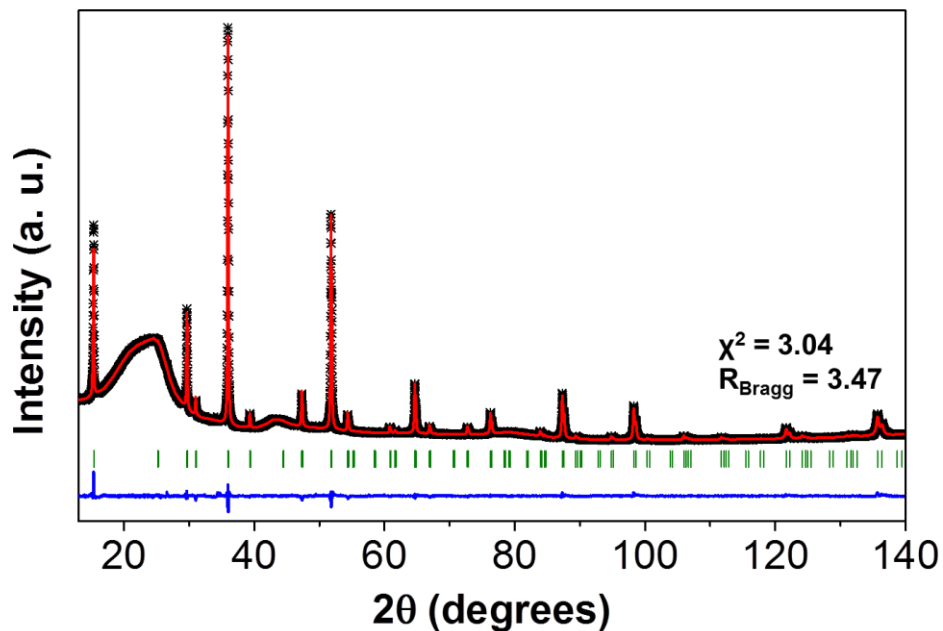


Fig. S8 XRD Rietveld refinement fit of partially discharged $\text{Mg}_{0.53}\text{Cu}_{0.1}\text{Ti}_2\text{S}_4$. (Black crosses – experimental data, red lines – fitted data, blue line – difference map between observed and calculated data, green ticks – the $\text{Fd}\bar{3}\text{m}$ spinel phase). The broad hump is a background signal from the X-ray capillary.

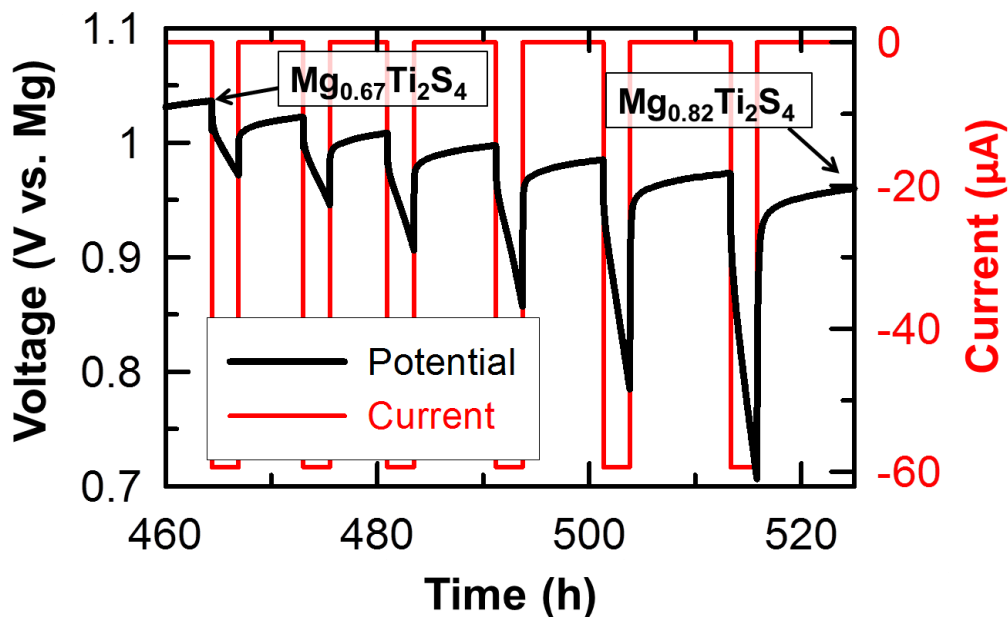


Fig. S9 Example galvanostatic intermittent titration profile near the end of discharge, showing the pronounced decrease in voltage during current-on periods, despite a seemingly constant decrease in the quasi-equilibrium potentials. This cell was run at 60°C in a three electrode configuration. Each current-on period used a C/200 (59.3 μA) rate for 2.5 h. The subsequent open circuit period was terminated when dE/dt (the slope) decreased to 0.1 mV/h.

References

1. N. Soheilnia, K. M. Kleinke, E. Dashjav, H. L. Cuthbert, J. E. Greedan, H. Kleinke, *Inorg. Chem.*, **2004**, 43, 6473 – 6478.
2. P. G. Bruce and M. Y. Saidi, *J. Solid State Chem.*, **1990**, 88, 411-418.
3. H. M. Rietveld, *J. Appl. Cryst.*, **1969**, 2, 65-71.
4. J. Rodríguez-Carvajal, *Physica B*, **1993**, 192, 55-69.
5. A. C. W. P. James and J. B. Goodenough, *Mat. Res. Bull.*, **1989**, 24, 143-155.
6. P. Lightfoot, F. Krok, J. L. Nowinski and P. G. Bruce, *J. Mater. Chem.*, **1992**, 2, 139-140.
7. O. Mizrahi, N. Amir, E. Pollak, O. Chusid, V. Marks, H. Gottlieb, L. Larush, E. Zinigrad and D. Aurbach, *J. Electrochem. Soc.*, **2008**, 155, A103-A109.
8. Periyapperuma, K., Tran, T. T., Trussler, S., Ioboni, D. & Obrovac, M. N. Conflat two and three electrode electrochemical cells. *J. Electrochem. Soc.*, **2014**, 161, A2182-A2187.
9. W. Weppner and R. A. Huggins, *J. Electrochem. Soc.*, 1977, **124**, 1569-1578.
10. D. Sheppard, R. Terrell and G. Henkelman, *J. Chem. Phys.*, **2008**, 128, 134106 – 134112.